

LASER INTERFEROMETER GRAVITATIONAL WAVE OBSERVATORY  
-LIGO-  
CALIFORNIA INSTITUTE OF TECHNOLOGY  
MASSACHUSETTS INSTITUTE OF TECHNOLOGY

<b>Technical Note</b>	<b>LIGO-T040177- 00- E</b>	Sep/10/04
-----------------------	----------------------------	-----------

<p style="text-align: center;"><b>Mode mismatch and sideband imbalance in LIGO I PRM</b></p>
--

Hiro Yamamoto / Caltech
-------------------------

This is an internal working note  
of the LIGO Project.

**California Institute of Technology**  
**LIGO Project – MS 18-34**  
**Pasadena CA 91125**  
Phone (626) 395-2129  
Fax (626) 304-9834  
E-mail: [info@ligo.caltech.edu](mailto:info@ligo.caltech.edu)

**Massachusetts Institute of Technology**  
**LIGO Project – NW17-161**  
**Cambridge, MA 01239**  
Phone (617) 253-4824  
Fax (617) 253-7014  
E-mail: [info@ligo.mit.edu](mailto:info@ligo.mit.edu)

WWW: <http://www.ligo.caltech.edu>

## **ABSTRACT**

The sideband imbalance and the mode mismatch in the LIGO I Power Recycled Michelson Cavity is studied using the Modal Model and the FFT program.

In this note, it is shown that the carrier is insensitive to the curvature mismatch of the field wave front and the ITM mirror surface, while the sideband is much more sensitive and higher order modes are excited due to that mismatch.

The Gouy phase of these higher order modes are common to both upper and lower sidebands, while the phase due to the Shnupp asymmetry is differential, i.e., has opposite sign, for the two sidebands. Because of this difference, as the mode mismatch in the Michelson becomes larger, the imbalance becomes larger. This effect is visible only when the curvature mismatch on two ITMs are different.

It is also shown that the curvature of the as-built LIGO BS surface can contribute to enhance the sideband imbalance.

## 1. INTRODUCTION

LIGO I performance has been improved by the thermal compensation system (TCS). By experience, it has been found that the performance is improved by heating two ITM mirrors differentially. One possible explanation is the improvement of the balance of upper and lower sidebands. The mechanisms of the cause of this balance or imbalance is not well known.

In this note, the effect of the curvature mismatch between the beam wave front and the mirror surface on two ITMs is studied and the imbalance of two sidebands caused by the thermal heating is discussed.

The BS curvature of the LIGO IFOs are much smaller than the specification. The requirement in the order form is that the curvature should be larger than 720km for the convex case, while the actual curvature of the delivered mirror surface of the LHO4k mirror is 200km, LLO4k 160km and LHO2k is 80km. It is shown that this BS curvature also induces the sideband imbalance. Because of this, it is possible that two ITMs need to be heated differentially in order to compensate the imbalance due to the BS curvature.

First, the mode decomposition due to curvature change is derived. Using this formula, the difference between the carrier and sidebands fields are discussed when reflected by a FP cavity with ITM whose surface curvature does not match with the field. When the TEM00 mode of carrier is reflected by this cavity, the major effect is an additional phase proportional to the size of mismatch, and no higher order modes are excited.

$$E_{ref}^{CR} = Exp(-i\alpha)E_{00} + O(\alpha^2)E_{mn}$$

On the contrary, when the TEM00 mode of a sideband is reflected, higher order modes are excited in addition to the same phase change as the carrier.

$$E_{ref}^{SB} = Exp(-i\alpha)(E_{00} - i\frac{\alpha}{\sqrt{2}}(E_{02} + E_{20})) + O(\alpha^2)E_{mn}$$

Because of this difference, the response of the locked IFO is different for the carrier and sidebands. Even when the curvature mismatch exists, the carrier is not affected almost at all, while sidebands experience the effects of PRM degeneracy.

For a sideband field which does not resonate in the long arm cavity, the ITM behaves as a perfect reflector. Using a simple FP cavity formed by RM and ITM, the effect of the curvature mismatch on the sideband imbalance is studied. When the curvature of the beam does not match with the curvature of ITM mirror surface, higher modes are excited when the field is reflected by ITM. Once excited, it is enhanced by a propagator with a form of

$$\frac{1}{1 - r_{RM}r_{ITM}Exp(-i2 \cdot \delta L \cdot k_{SB} + i2(m+n)\eta_{00})}$$

In this formula, the first phase comes from the Shnupp asymmetry  $dL$  and the second term is the Gouy phase between RM and ITM. The first term has an opposite sign for the upper and lower sideband ( $k_{SB} = \pm 2\pi / \lambda_{RF}$ ), while the Gouy phase is common to both. Because of this difference, the enhancement of excited higher order modes for upper and lower sidebands are different in the PRM. With the parameters for LIGO I cavity, it is shown that an observable amount of sideband difference is caused with typical size of the curvature

mismatch. As the curvature mismatch becomes larger, the excitation of higher order mode becomes larger, so the imbalance becomes larger.

When two ITMs are equally mode mismatched, the upper sideband is more populated in the inline PRM cavity while the lower sideband is more populated in the offline PRM cavity by the same amount. Because of this, the imbalance is not observable. But when the sizes of the mismatch of two ITMs are different, the imbalance on one PRM cavity becomes more dominant than the other, and the imbalance is observed.

When the size of the BS surface curvature is not infinite, the beam curvature reflected toward ITM becomes different than the transmitted field. Due to this, the effect of the BS curvature appears as if two ITMs have different curvature mismatching. One major difference between the genuine ITM curvature mismatch and the effect of the BS curvature is the astigmatism. The curvature mismatch of ITMs does not introduce any astigmatism, while the effect caused by the BS curvature is astigmatic because of the 45 degree tilt.

The FFT program uses plane wave propagation technique to study the details of the IFO effects, and can handle details more precisely than the Modal Model calculation with small number of modes. The FFT program was used to simulate various cases and all the conclusions above based on the modal model have been found to be consistent with the FFT simulation.

## **2. KEY WORDS**

sideband imbalance, mode matching, thermal heating, modal model, FFT

## **3. Basics**

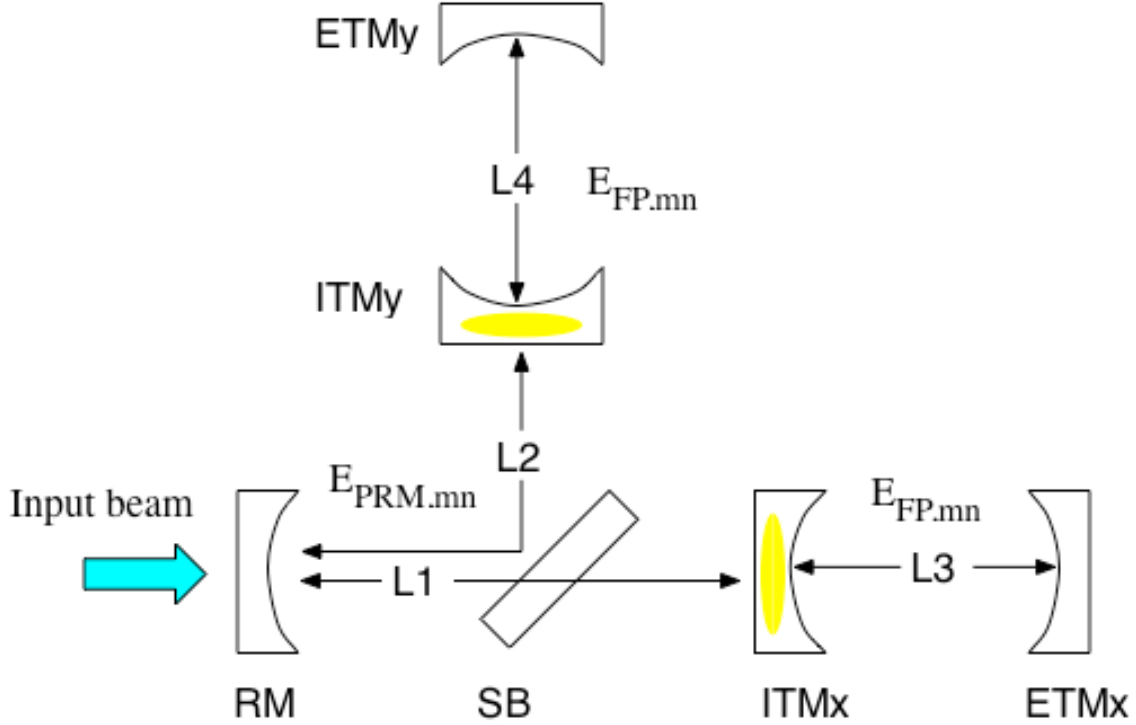


Fig.1 Schematics of IFO

Figure 1 is the schematics of the LIGO Interferometer. Two modal model bases are defined,  $E_{PRM}$  and  $E_{FP}$ .  $E_{PRM}$  is a mode base specified by RM and ITMx with optimal thermal distortion, where optimal means the amount of distortion expected at the design input power with the absorption measured using the sample piece. The effective refractive index (see appendix 1) for the optimal heating,  $n_h$ , is 0.96, and the curvature of ITM seen from the PRM side is  $ROC(ITM)/n_h$ , or 14.5km. Another mode  $E_{FP}$  is defined by ITM and ETM. The thermal distortion in LIGO I does not affect the surface geometry. These two mode bases do not depend on the actual thermal distortion in ITMs which may not be optimal.

The input beam TEM00 mode is set so that it becomes  $E_{PRM,00}$  after going through RM, which is not affected much by the thermal effect.  $E_{PRM,mn}$  becomes  $E_{FP,mn}$  when ITMs are optimally heated. When ITMs are not heated optimally, higher order modes are excited by the interaction with ITMs.

#### 4. Reflection by a FP cavity

In this section, the effect of the curvature mismatch on the reflection of carrier and sideband fields. Figure 4 shows interaction of fields.  $E_0$  is the input field to the FP cavity. Evolution is analyzed when  $E_0$  is TEM00 of  $E_{PRM}$  base, which means that the beam curvature on ITM is  $ROC(ITM)/n_h$ .

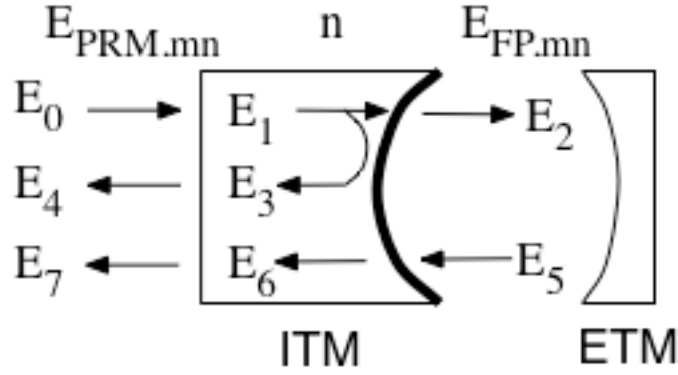


Fig. 4 Reflection by FP

$E_0$  goes through the ITM lens to become  $E_1$ , whose curvature is

$$\frac{1}{ROC(E_1)} = -\frac{1-n+n_h}{ROC(ITM)}$$

The curvature of the reflected field,  $E_3$ , is

$$\frac{1}{ROC(E_3)} = \frac{1+n-n_h}{ROC(ITM)}$$

$E_3$  goes through ITM lens to become  $E_4$ , whose curvature is

$$\frac{1}{ROC(E_4)} = \frac{2n-n_h}{ROC(ITM)}$$

So, the reflected field  $E_4$  is a TEM<sub>00</sub> with the same beam size as  $E_{PRM}$  on ITM, while the radius is different. Using the formula in Appendix 2,  $E_4$  can be expressed using the  $E_{PRM}$  base with the following  $\alpha$ .

$$\alpha_4 = \frac{z_{PRM}}{z_{0\ PRM}} \left( \frac{n}{n_h} - 1 \right) = \frac{z_{FP}(\leftarrow)}{z_{0\ FP}} (n - n_h)$$

$z$  and  $z_0$  with suffix PRM and FP are the distance to waist and Rayleigh range using the  $E_{PRM}$  and  $E_{FP}$  base.  $z(\leftarrow)$  means the distance to waist of the diverging beam, and is positive, while  $z(\rightarrow)$  used below is that of the converging beam and is negative. Using this  $\alpha$ ,  $E_4$  can be expressed using the  $E_{PRM}$  based as follows.

$$E_4 = r_{ITM} \left( \frac{1}{1+i\alpha_4} E_{00} - \frac{i\alpha_4/\sqrt{2}}{(1+i\alpha_4)^3} (E_{02} + E_{20}) + O(\alpha_4^2) \right)$$

This shows that the promptly reflected field is affected by the curvature mismatch.

$E_1$  goes through the HR coating and becomes  $E_2$  whose curvature is the same as  $E_1$ . This field can be expressed using  $E_{FP}$  base whose curvature on ITM is  $ROC(ITM)$ . The  $\alpha$  parameter for this expansion is

$$\alpha_2 = -\frac{z_{FP}(\rightarrow)}{2z_{0\ FP}} (n - n_h) = \frac{z_{FP}(\leftarrow)}{2z_{0\ FP}} (n - n_h) = \frac{1}{2} \alpha_4$$

and the field  $E_2$  is

$$E_2 = t_{ITM} \left( \frac{1}{1+i\alpha_2} E_{00} - \frac{i\alpha_2/\sqrt{2}}{(1+i\alpha_2)^3} (E_{02} + E_{20}) + O(\alpha_4^2) \right)$$

When the  $E_{FP,00}$  mode is resonant in the FP cavity, only E00 contributes to the leak through the ITM back into reflected direction. In other words, E5 can be approximated by

$$E_5 = \frac{-r_{ETM} \cdot t_{ITM}}{1 - r_{ITM} r_{ETM}} \frac{1}{1 + i\alpha_2} E_{00}$$

When E5 goes through ITM lens, the curvature changes from  $ROC(ITM)$  to

$$\frac{1}{ROC(E7)} = \frac{n}{ROC(ITM)}$$

E7 can be expanded using the following  $\alpha$ .

$$\alpha_7 = \frac{z_{FP}(\leftarrow)}{2z_{0,FP}}(n - n_h) = \alpha_2 = \frac{1}{2}\alpha_4$$

$$E_7 = \frac{-r_{ETM} \cdot t_{ITM}^2}{1 - r_{ITM} r_{ETM}} \frac{1}{1 + i\alpha_2} \left( \frac{1}{1 + i\alpha_7} E_{00} - \frac{i\alpha_7 / \sqrt{2}}{(1 + i\alpha_7)^3} (E_{02} + E_{20}) + O(\alpha_7^2) \right)$$

All three  $\alpha$ s representing curvature mismatch are essentially the same.

$$2\alpha_2 = 2\alpha_7 = \alpha_4 \equiv \alpha$$

In the following, to simplify the argument, the following approximation is used.

$$r_{ITM} = 1, \quad \frac{-r_{ETM} \cdot t_{ITM}^2}{1 - r_{ITM} r_{ETM}} = -2$$

Sideband fields do not resonant in the arm, so the SB reflection is represented by the expression for E4.

$$E_{SB} = \frac{1}{1 + i\alpha} E_{00} - \frac{i\alpha / \sqrt{2}}{(1 + i\alpha)^3} (E_{02} + E_{20}) + O(\alpha^2)$$

The reflected field of carrier is the sum of two components, the prompt reflection, E4, and the leak from the FP cavity, E7.

$$\begin{aligned} E_{CR} &= \frac{1}{1 + i\alpha} E_{00} - \frac{i\alpha / \sqrt{2}}{(1 + i\alpha)^3} (E_{02} + E_{20}) + O(\alpha^2) \\ &\quad - 2 \frac{1}{1 + i\alpha / 2} \left( \frac{1}{1 + i\alpha / 2} E_{00} - \frac{i\alpha / 2 / \sqrt{2}}{(1 + i\alpha / 2)^3} (E_{02} + E_{20}) + O(\alpha^2) \right) \\ &= -\frac{1}{1 + i\alpha} E_{00} + O(\alpha^2) \end{aligned}$$

When you compare  $E_{SB}$  and  $E_{CR}$ , the following points are observed to the first order of mismatch.

- (1) 00 components are affected equally
- (2) For CR, only 00 mode is reflected, and higher order modes are not excited
- (3) For SB, higher order modes are produced in the reflection which is proportional to the curvature mismatch

## 5. Coupled cavity with mode mismatch

In this section, a coupled cavity consisted of RM, ITM and ETM is studied. When the ITM is optimally heated, the input beam mode matches with this coupled cavity system. When the ITM is not optically heated, the interaction with the ITM introduces mode mismatch.

When the arm consisted of ITM and ETM is locked to the carrier 00 mode,  $E_{FP,00}$ , the carrier 00,  $E_{PRM,00}$ , reflected by this FP arm does not have higher order modes, and the net effect is the phase change due to the curvature mismatch,

$$E_{CR}^{ref} \approx -\frac{1}{1+i\alpha} E_{PRM,00} \approx -Exp(-i\alpha) E_{PRM,00}$$

When the length of the short cavity consisted of RM and ITM is adjusted to compensate this phase change,  $i\alpha$ , then the coupled cavity satisfies the lock condition of the carrier 00, i.e., all phase changes through propagations in the short and long cavities satisfy the resonant condition and no higher order modes are excited.

When the FFT program is used to simulate the LIGO IFO with symmetric parameters (see Appendix 4), the following cavity length changes resulted under different ITM thermal states. In all cases, the arm length did not change.

dL \ n(x)-n(y)	0.96-0.96	0.96-1.1	1.1-0.96	1.0-1.0	1.1-1.1	1.2-1.2
RM-ITMx	0	0	$-\alpha(1.1)$	$-\alpha(1.0)$	$-\alpha(1.1)$	$-\alpha(1.2)$
RM-ITMy	0	$-\alpha(1.1)$	0	$-\alpha(1.0)$	$-\alpha(1.1)$	$-\alpha(1.2)$

Table 1. Michelson cavity length change due to mismatch

The first row shows the pair of refractive indexes of ITMx and ITMy. 0.96 is value for optimal heating. The second and third rows show the length change of two Michelson cavity length in units of  $\lambda(CR)/4\pi$ . Numerical values of various  $\alpha$ s are given in Appendix 4. From this one, one can see that the cavity lock using the carrier can be easily explained by the argument in the previous section. I.e., on reflection, CR 00 acquires phase  $-\alpha$ , and the corresponding cavity length is adjusted to compensate this phase due to curvature mismatch.

n(x) / $\alpha$	1.0 / 0.011	1.1 / 0.039	1.2 / 0.067
Upper / Lower	1.07	1.74	2.60

Table 2. Sideband imbalance in one coupled cavity

## 6. Michelson cavity with mismatch

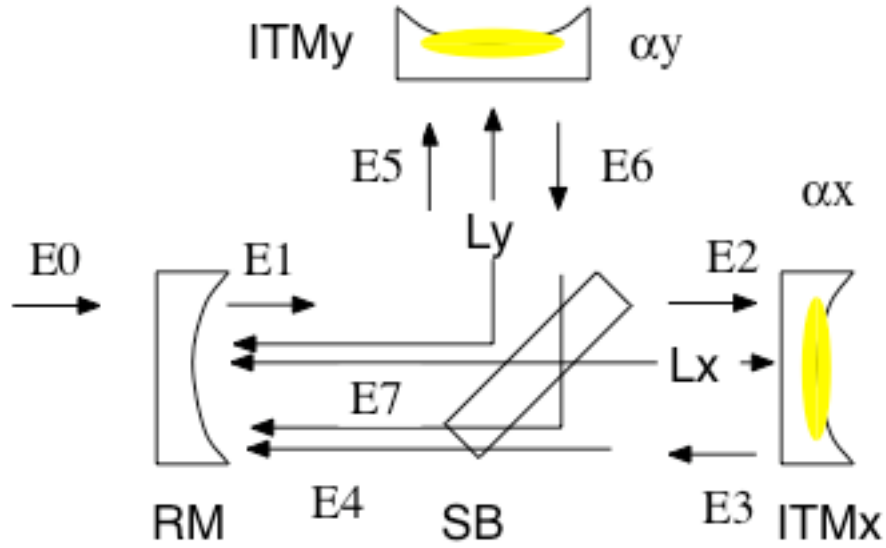


Fig. 5 Michelson cavity with curvature mismatch

	FFT			Modal Model 00+02+20		
	Upper SB	Lower SB	Up/Low	Upper	Lower	Up/Low
0.96-0.96	25.8	25.8	1	25.9	25.9	1
1.1-0.96	22.1	20.1	1.10	18.3	16.7	1.10
1.2-0.96	17.2	14.8	1.16	12.6	9.8	1.29

Table 3. Sideband imbalance in Michelson cavity

### Appendix 1 Effective Refractive Index

When a LIGO mirror is heated by laser beam, several effects adds non uniform optical path length change in the substrate. When this additional effect can be approximated by a thin lens, the combined system can be represented by one mirror with different refractive index.

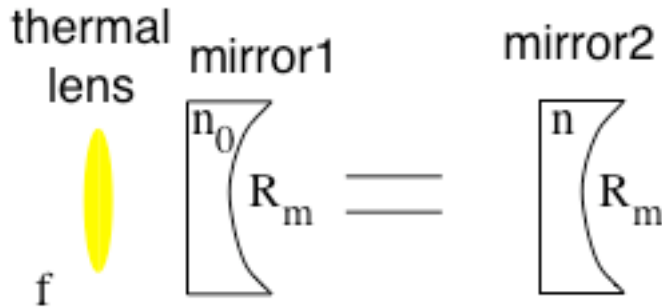


Figure A1 Equivalent single mirror

The left hand side represents an actual system. Mirror1 has a curvature of  $R_m$  on the HR side and the refractive index of the substrate is  $n_0$ . The thermal distortion effect is approximated by a thin lens with the focal length of  $f$ . The right hand side is a single mirror with a refractive index  $n$ . When  $n$  is chosen to be,

$$n = n_0 - \frac{R_m}{f}$$

the focal length of these two setup become the same. Also, the physical curvature of the HR side are equal. So, use of an effective refractive index is a very convenient way to simulate a mirror with thermal lensing effect.

The approximation of the actual thermal distortion by a simple lens is discussed in the other note (LIGO-G040328). The fit of the thermal distortion calculation using FEM gives the following f number.

$$f = \frac{1.7km}{P_{abs}(W)}$$

This is a result for the LIGO I ITM mass, and Power is the total laser power absorbed to heat the mass. With the average ITM curvatures of LIGO LHO4k IFO,  $R_m=13.9km$ , the effective refractive index is given as following.

$$n = n_0 - 8.2 \cdot P_{abs}(W) = 1.45 - 8.2 \cdot P_{abs}(W)$$

In this approximation, the optimal absorption power corresponds to 60mW.

## Appendix 2. Mode coupling due to curvature mismatch

Details of mode couplings in various cases are discussed in LIGO-T990081. In this appendix, the coupling due to the curvature mismatch is summarized. In Fig.A2, two mode bases are shown. Both are characterized by the beam curvature and the beam size in the plane marked by a dotted line. Both have the same beam size, but curvatures are different.

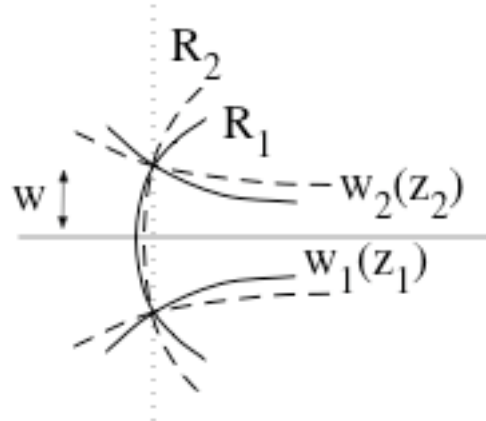


Fig. A2 Two modes with different curvature

Each eigenstate using the base defined by  $(w, R_2)$  can be expressed using the base defined by  $(w, R_1)$  by the following formula.

$$TEM_{m_2 n_2}(x, y : w^x, R_2^x, w^y, R_2^y) = \sum_{m_1, n_1} M_{m_2, m_1}(\alpha_x) \cdot M_{n_2, n_1}(\alpha_y) \cdot TEM_{m_1 n_1}(x, y : w^x, R_1^x, w^y, R_1^y)$$

The coupling coefficient  $M_{m_1 m_2}(\alpha)$  is given as follows.

$$\begin{aligned}
M_{m_2 m_1}(\alpha) &= \int dx \cdot u_{m_2}(x : w, R_2) \cdot u_{m_1}(x : w, R_1)^* \\
&= \frac{1}{\sqrt{\pi 2^{m_1+m_2} m_1! m_2!}} \int d\xi H_{m_1}(\xi) H_{m_2}(\xi) \text{Exp}[-\xi^2(1+i\alpha)] \\
\alpha &= \frac{k \cdot w^2}{4} \left( \frac{1}{R_2} - \frac{1}{R_1} \right) = \frac{z}{2z_0} \left( \frac{R_1}{R_2} - 1 \right)
\end{aligned}$$

In the expression of  $\alpha$ ,  $z$  is the distance to the waist and  $z_0$  is the Rayleigh range for the mode base defined by  $w$  and  $R_1$ .

In the following, a few matrix elements are shown.

$m_1 \setminus m_2$	0	1	2
0	$\frac{1}{(1+i\alpha)^{1/2}}$	0	$\frac{-i\alpha}{\sqrt{2}(1+i\alpha)^{3/2}}$
1	0	$\frac{1}{(1+i\alpha)^{3/2}}$	0
2	$\frac{-i\alpha}{\sqrt{2}(1+i\alpha)^{3/2}}$	0	$\frac{1-\alpha^2/2}{(1+i\alpha)^{5/2}}$

Table A1. Mode coupling coefficients

An important point is that the diagonal element, like  $M_{00}$ , has phase  $-i\alpha$  due to the curvature mismatch. Because of that, a cavity length needs to be adjusted proportional to the curvature mismatch to make the cavity resonant.

### Appendix 3. Field in a mode mismatched FP cavity

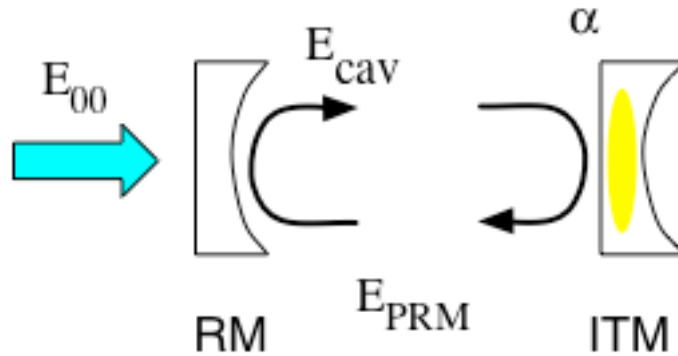


Fig. A3 FP cavity with curvature mismatch

In this appendix, the mode content of a field in a FP cavity which does not mode match to the input beam. The input beam in Fig.A3 becomes  $E_{PRM,00}$  in the FP cavity formed by RM and ITM, i.e., the input beam mode matches with the FP cavity when the ITM is optimally heated. The magnitude of the mismatch is represented by  $\alpha$ .

Using the mode coupling matrix derived in Appendix 2, the stationary field in the FP cavity is given as follows.

$$E_{cav} = \frac{t_{RM} \cdot E_{in}}{(1-R)(1+C_0 \cdot \alpha^2)} (E_{PRM,00} - i \cdot \alpha \cdot C_2 \cdot (E_{PRM,02} + E_{PRM,20})) + O(\alpha^3)$$

where various coefficients are defined as follows using the Gouy phase  $\eta$ .

$$R = R_0 \cdot \text{Exp}[i\phi_{CR,00} + i\phi], \quad R_0 = r_{RM} \cdot r_{ITM}$$

$$\phi_{CR,00} = -2k_{CR}L + 2\eta - \arctan(\alpha)$$

$$\phi_{mix} = \frac{1}{2} \cot(2\eta) \cdot \alpha^2$$

$$\phi = -2k_{SB}L + 2(n+m)\eta + \phi_{mix}$$

$$C_0 = \frac{(1 - i \cdot \cot(2\eta)) \cdot R}{2(1 - \text{Exp}(i4\eta)R)}$$

$$C_2 = \frac{\text{Exp}(i \cdot 2\eta)}{\sqrt{2}(1 - \text{Exp}(i \cdot 4\eta)R)}$$

There are two points to note. One is that the curvature mismatch introduces a phase proportional to  $\alpha$ , and the cavity length needs to be adjusted to compensate this phase due to the curvature mismatch. Second is the lock condition. When the FP arm is attached, the reflection of CR 00 does not have higher order mode produced. The phase  $\phi_{mix}$  comes from the down coupling, i.e., 00  $\rightarrow$  02/20  $\rightarrow$  00. So, the carrier does not have this term. Because of that, the lock condition of CR 00 is  $\phi_{CR,00} = (n+1/2)\pi$ .

The total power in the cavity is

$$P(00,02,20) = P_0(1 - \alpha^2 P_2)$$

$$P_0 = \frac{T_{RM}}{(1 - 2R_0 \cos(\phi) + R_0^2)}$$

$$P_2 = \frac{R_0 \sin(2\eta + \phi) - (1 - R_0^2) \text{Sin}(2\eta)}{\sin(2\eta)(1 - 2 \cos(4\eta + \phi)R_0 + R_0^2)}$$

From the expression of C0 and Power, one can see that the perturbative calculation does not work when  $\alpha^2/\sin(2\eta)$  is not small. For a near degenerate cavity whose Gouy phase change is small, many modes can equally resonate. Small curvature mismatch induces many modes and many modes excited need to be included in the calculation.

#### Appendix 4. LIGO Parameters

Two sets of LIGO parameters are used in this calculation. The as-built set uses the as-built values of curvatures, transmittance, losses and the mirror thickness is included. The

symmetric set uses the average values of inline and offline arms for both arms, and the mirror thickness is set to zero. The Shnupp asymmetry is retained.

Symmetric LIGO

RF = 24.482MHz

Power reflection

RM : 0.9729, ITM<sub>x</sub> = ITM<sub>y</sub> = 0.9722

ROC in m

RM = 14400, ITM<sub>x</sub> = ITM<sub>y</sub> = 13920, ETM<sub>x</sub> = ETM<sub>y</sub> = 7290

Cavity lengths in m

RM-BS = 4.397, BS-ITM<sub>x</sub> = 4.9765, BS-ITM<sub>y</sub> = 4.5975, ITM<sub>x</sub>-ETM<sub>x</sub> = ITM<sub>y</sub>-ETM<sub>y</sub> = 3995.055

$2k_{SB} L(\text{RM-ITM}_x) = 3\pi + \phi_{\text{Snp}}$ ,  $2k_{SB} L(\text{RM-ITM}_y) = 3\pi - \phi_{\text{Snp}}$ ,  $\phi_{\text{Snp}} = 0.195$

Mode base in PRM

$z_0$ (Rayleigh range in PRM) = 3600 m,  $z(\text{ITM})$  : distance between ITM to waist = 957 m

Gouy phase in PRM

$\eta(\text{RM-ITM}_x) = 2.43\text{e-}3$ ,  $\eta(\text{RM-ITM}_y) = 2.33\text{e-}3$

mismatch parameter for different effective refractive index of ITM

$\alpha(0.959) = 0$ ,  $\alpha(1.0) = 0.011$ ,  $\alpha(1.1) = 0.039$ ,  $\alpha(1.2) = 0.067$